J Physiol 588.24 (2010) pp 5049–5063

The Journal of Physiology

Loss of PDZ-adaptor protein NHERF2 affects membrane localization and cGMP- and [Ca^{2+}]- but not cAMP-dependent regulation of Na^+/H^+ exchanger 3 in murine intestine

Mingmin Chen[1], Ayesha Sultan[1], Ayhan Cinar[1], Sunil Yeruva[1], Brigitte Riederer[1], Anurag Kumar Singh[1], Junhua Li[1,2], Janina Bonhagen[1], Gang Chen[2], Chris Yun[3], Mark Donowitz[4], Boris Hogema[5], Hugo deJonge[5] and Ursula Seidler[1]

[1] *Department of Gastroenterology, Hepatology and Endocrinology, Hannover Medical School, Hannover 30625, Germany*
[2] *Institute of Organ Transplantation, Tongji Hospital, Tongji Medical College, Huazhong University of Science and Technology, Wuhan, Hubei, China*
[3] *Departments of Medicine and Physiology, Emory School of Medicine, Atlanta, GA, USA*
[4] *Departments of Medicine and Physiology, Johns Hopkins University School of Medicine, Baltimore, MD, USA*
[5] *Department of Biochemistry, Erasmus University Medical Center, Rotterdam, The Netherlands*

Trafficking and regulation of the epithelial brush border membrane (BBM) Na^+/H^+ exchanger 3 (NHE3) in the intestine involves interaction with four different members of the NHERF family in a signal-dependent and possibly segment-specific fashion. The aim of this research was to study the role of NHERF2 (E3KARP) in intestinal NHE3 BBM localization and second messenger-mediated and receptor-mediated inhibition of NHE3. Immunolocalization of NHE3 in WT mice revealed predominant microvillar localization in jejunum and colon, a mixed distribution in the proximal ileum but localization near the terminal web in the distal ileum. The terminal web localization of NHE3 in the distal ileum correlated with reduced acid-activated NHE3 activity (fluorometrically assessed). NHERF2 ablation resulted in a shift of NHE3 to the microvilli and higher basal fluid absorption rates in the ileum, but no change in overall NHE3 protein or mRNA expression. Forskolin-induced NHE3 inhibition was preserved in the absence of NHERF2, whereas Ca^{2+} ionophore- or carbachol-mediated inhibition was abolished. Likewise, *Escherichia coli* heat stable enterotoxin peptide (STp) lost its inhibitory effect on intestinal NHE3. It is concluded that in native murine intestine, the NHE3 adaptor protein NHERF2 plays important roles in tethering NHE3 to a position near the terminal web and in second messenger inhibition of NHE3 in a signal- and segment-specific fashion, and is therefore an important regulator of intestinal fluid transport.

(Resubmitted 31 August 2010; accepted 11 October 2010; first published online 20 October 2010)
Corresponding author U. Seidler: Department of Gastroenterology, Hepatology and Endocrinology, Hannover Medical School, Carl-Neuberg-Straße 1, D-30625 Hannover Germany. Email: seidler.ursula@mh-hannover.de

Abbreviations BBM, brush border membrane; NHE3, Na^+/H^+ exchanger isoform 3.

Introduction

The Na^+/H^+ exchanger isoform 3 (NHE3) is responsible for a major part of intestinal NaCl absorption (Zachos *et al.* 2005). When it was cloned from rabbit intestine and expressed in the Na^+/H^+ exchanger-deficient fibroblast cell line PS120, cAMP analogues failed to inhibit NHE3 transport rate (Tse *et al.* 1991). Subsequently, a PDZ-adaptor protein interacting with NHE3 was cloned from a human lung library (Yun *et al.* 1997). This protein was called NHE3 kinase A regulatory protein (E3KARP), because coexpression with NHE3 restored the cAMP-mediated NHE3 inhibition (Yun *et al.* 1997; Lamprecht *et al.* 1998; Zizak *et al.* 1999). The same effect was seen when the highly similar PDZ-protein NHERF1 was coexpressed with NHE3. E3KARP was found to be identical to the NHERF1 homologue NHERF2 (Hall *et al.* 1998). NHERF2, but not NHERF1, was later demonstrated to be essential for Ca^{2+}- and cGMP-mediated inhibition of NHE3 by facilitating the

DOI: 10.1113/jphysiol.2010.198721

formation of the NHE3–NHERF2–α-actinin-4 complex that promotes $[Ca^{2+}]_i$-dependent NHE3 oligomerization and endocytosis (Kim *et al.* 2002), and by bringing cGMP-dependent protein kinase type II (cGKII) into close proximity to NHE3, which is necessary for cGMP-dependent NHE3 inhibition (Cha *et al.* 2005).

Investigating the recently generated NHERF1 deficient mice resulted in the surprising finding that whereas NHERF1 proved essential for cAMP-mediated NHE3 inhibition in the kidney, this function was not affected in the NHERF1 deficient intestine (Murtazina *et al.* 2007; Broere *et al.* 2009). In contrast, another member of the NHERF family, PDZK1, was shown to be of particular importance for cAMP-mediated inhibition in the murine intestine (Cinar *et al.* 2007; Hillesheim *et al.* 2007; Broere *et al.* 2009). Thus, it appeared that the action of the NHERFs on NHE3 may be cell type as well as signal specific. These findings prompted us to study the localization and agonist-mediated regulation of NHE3 in the different intestinal segments of the recently generated NHERF2 deficient mouse model (Broere *et al.* 2007).

Methods

Chemicals

Chemicals were obtained from Sigma (Deisenhofen, Germany) or Merck (Darmstadt, Germany) at tissue culture grade or the highest grade available, unless indicated otherwise. Hoe 642 and S1611 were kindly provided by Sanofi-Aventis (Frankfurt, Germany). 4-Bromo-A23187 was purchased from Biomol (Hamburg, Germany) and *E. coli* enterotoxin STp was from Bachem (Weil am Rhein, Germany). Nigericin and 2,7-biscarboxyethyl-5(6)-carboxyfluorescein (BCECF) were purchased from Molecular Probes (Leiden, the Netherlands). The antibodies used are specified in the appropriate Methods section.

Animal breeding

Nherf2$^{-/-}$ mice were originally generated from Lexicon genetics clone OST2298 (Broere *et al.* 2007) and were bred into a congenic FVB/N background in the animal facility of the Hannover Medical School under standardized light and climate conditions with access to water and chow *ad libitum*. Age- and sex-matched wild-type littermates were used as controls. The genotype was determined by PCR as previously described (Singh *et al.* 2009). The NHE3-deficient mouse strain had originally been generated by Schultheis *et al.* (1998) and had been bred for >10 generations at Hannover Medical School. Animal experiments followed approved protocols at the Hannover Medical School and were reviewed and approved by an independent committee on animal rights assembled by the local authorities for the regulation of animal welfare.

mRNA isolation and quantitative real-time PCR

mRNA was isolated from the different segments of murine intestine that were also functionally studied (see below). Isolation method, primers and PCR procedure have been described previously (Hillesheim *et al.* 2007; Broere *et al.* 2009).

In vivo intestinal fluid transport measurements

The measurements of fluid absorptive rates were performed via a single pass method, as described by us for the jejunum (Broere *et al.* 2009; Chen *et al.* 2010; Singh *et al.* 2010). The mice were anaesthetised by isoflurane inhalation, and blood pressure and ventilatory rate were continuously monitored using a PowerLab II-26 (ADInstruments, Spechbach, Germany). For jejunal perfusion, the inlet tube was inserted approx. 5–8 cm distal to the pylorus and a 5–7 cm segment was perfused; for the ileal perfusion, 5 cm of the ileum was used, with the distal end of the perfused segment 1–2 cm proximal to the ileocaecal valve; and for colon perfusion, the second part of the colon (not the haustrated, wide part of the proximal colon) was perfused with the distal end about 1 cm proximal to the anus. For colon perfusion, a higher perfusion speed ($30\ ml\ h^{-1}$) was chosen to prevent clogging of mucous material, and the fluid was recirculated with a precision pump (Minipuls Evolution; Gilson, Villiers, France) and constantly kept at 37°C in a water bath. At the end of the experiment, the mouse was killed by cervical dislocation while still under anaesthesia. Since the incision is made as small as possible, and exact determination of the length and the distance to pylorus of the perfused jejunal segment could only be made after killing of the mouse and excision of the gut, and therefore varies somewhat between experiments. S1611 was used to inhibit NHE3-mediated fluid absorption (Schwark *et al.* 1998; Bachmann *et al.* 2004; Cinar *et al.* 2007; Singh *et al.* 2010); in addition to the experiments performed in the cited studies, it was tested by us for potential inhibition of ENaC in distal colon of mice on a low salt diet, and NHE2 WT and KO mice, and found not to do so (X, Fang & J, Li, unpublished observations).

Ligated loop experiments in different segments of the small intestine

While the above described single pass perfusion techniques allow better control of acid/base balance during anaesthesia, a sequential assessment of basal and inhibitor-treated absorptive rates, and do not alter

luminal fluid pressure, they are less well suited to perform simultaneous fluid absorption measurements in different intestinal segments in the same mouse. Therefore, classic ligated loop experiments were also performed as previously described (Broere *et al.* 2009). In these experiments, the mice were anaesthetized with ketamine/xylazine (100 and 20 mg kg^{-1}, respectively, I.P.); 10–12 cm of proximal (approx. 5 cm from pylorus) and distal (approx. 17–20 cm from pylorus) and ileal (last 10–12 cm of small intestine) segments were ligated, and defined amounts of isotonic saline were injected into the ligated intestinal loops; the abdomen was closed, and the mice were kept in a humidified 37°C atmosphere for 1 h. Thereafter the mice were killed, the segments were removed, the fluid was removed and weighed, and the segment length was measured.

NHE3 distribution relative to the brush border membrane

Stained sections were imaged on the confocal microscope (Leica DM IRB with a TCS SP2 AOBS scan head equipped with a 405 nm laser for excitation of blue dyes). Sections from *Nherf2*$^{+/+}$ and *Nherf2*$^{-/-}$ jejunum, ileum and colon were imaged with identical confocal settings. A detailed method description is given in online Supplemental Material. In this paper, we call the location of the peak of the actin signal which is also the innermost part of the apical actin stain the 'terminal web', because PEPT1 is seen in the complete microvillar region but not in this part (Chen *et al.* 2010), whereas NHE3 can be found in the innermost part of the actin band (likely to be in recycling endosomes within the terminal web; Hansen *et al.* 2009). We did not distinguish technically between the base of the microvilli and the terminal web, but looking at the localization of NHE3 in relation to F-actin, and comparing that to the ultrastructural architecture of the microvilli and the terminal web, we have to conclude that most likely a part of NHE3 is in the terminal web region and not just at the base of the microvilli (Hirokawa *et al.* 1982). However, since this was not the focus of the study (since a difference between NHE3 at the base of the microvilli or the recycling endosomes would not have an impact on the interpretation of our current data), a more detailed ultrastructural localization of NHE3 was not attempted.

Intestinal brush border membrane preparation

The preparation of jejunal and ileal brush border membranes (BBMs) was performed by the divalent cation precipitation technique similar to previously published protocols (Hillesheim *et al.* 2007), with modifications as described in the Supplemental Material.

Immunoblot analysis

BBM was denatured in sample buffer at 65°C for 10 min, resolved on a 10% SDS-polyacrylamide gel and transferred to PVDF membrane (GE Healthcare, Little Chalfont, UK). Blots were blocked with 5% skimmed milk and first incubated with rabbit anti-rat NHE3 (Alpha Diagnostic, San Antonio, TX, USA, NHE31-A; 1:2500) or rabbit anti-rat villin (H-60, Santa Cruz Biotechnology, Santa, Cruz, CA, USA; 1:2500) for 2 h at room temperature (RT) followed by horseradish peroxidase (HRP) conjugated anti-rabbit antibody (KPL, Inc., Gaithersburg, MD, USA; 1:10,000) for 1 h at RT. Blots were subsequently developed by using ECL (GE Healthcare) and the signal was quantified by TotalLab software (TotalLab Ltd, Newcastle upon Tyne, UK). In case of excessive villin signal the membrane was stripped by incubating with stripping buffer (62 mM Tris, pH 6.8, 2% SDS, 0.7% β-mercaptoethanol) at 50°C for 30 min, washed and re-blocked with 5% skimmed milk, followed by the above specified Western protocol.

Preparation of isolated intestinal villi for fluorometry

For measuring pH_i in isolated jejunal and ileal villi, the proximal jejunum (approximately 6 cm distal to the pylorus), the ileum (approx. 8 cm proximal to the ileocaecal junction) and the distal ileum (approx. 1 cm proximal to the ileocaecal junction) were removed and immediately placed in ice-cold Ringer solution (solution composition in mM: 147 NaCl, 4 KCl, 2.2 $CaCl_2$ in 500 μM DTT to prevent mucus clogging of the villi, pH 7.4). The method is described in detail in Chen *et al.* (2010).

Fluorometric pH_i measurements in intact villi

The method for pH_i measurement and assessment of acid-activated NHE3 activity in intact microdissected jejunal villi has recently been described in Chen *et al.* (2010) and was performed identically here. Intrinsic buffering capacity was determined in the villous enterocytes of each studied intestinal segment and the curves are given in the Supplemental Material. Calibration of the 440/495 ratio was performed as described in Hegyi *et al.* (2004). For the calculation of proton extrusion rates, the intrinsic buffer capacity was determined for jejunal (shown in Chen *et al.* 2010), and ileal (see Suppl. Fig. 2) enterocytes within microdissected villi, as described in Chen *et al.* (2010). The buffer capacity of colonic crypts had previously been reported in Bachmann *et al.* (2003). Although we did not construct a full buffer curve for NHERF2 knockout enterocytes of the different intestinal segments, we did perform individual buffer capacity measurements and these values were in the same range as those of the WT mice.

Preparation of colonic crypts and fluorometric pH_i measurements

The isolation of murine colonic crypts and pH_i recovery from an ammonium prepulse-induced acidification were performed exactly as previously described in Cinar *et al.* (2007) and Broere *et al.* (2009).

Statistics

Data are presented as means ± S.E.M. The Mann–Whitney rank-sum, Student's *t* test and ANOVA were used for statistics, where appropriate, and values of $P < 0.05$ were considered significant.

Results

In vivo fluid absorption in the different segments of the intestine of anaesthetized NHERF2-deficient and WT mice

NHE3 is involved in electroneutral NaCl uptake, resulting in fluid absorption. To obtain an indication as to whether NHE3 regulation is altered in NHERF2-deficient mice, we first measured fluid absorption by single pass experiments in the jejunum, ileum and mid colon of anaesthetized NHERF2 KO and WT mice (segments defined in Methods). Interestingly, NHERF2 ablation resulted in significantly increased absorptive rates in the ileum (Fig. 1*A* and *C*), but not the jejunum and colon (Fig. 1*A* and *C*). The NHE3 inhibitor S1611 almost fully inhibited fluid absorption in all segments, indicating that NHE3 is the major Na^+ absorptive transporter in the absence of nutrients in the murine small and large colon (Fig. 1*B*).

Fluid absorption was also studied simultaneously in the same mouse (ligated loop experiments) in proximal and distal jejunal, as well as ileal loops of NHERF2 WT and KO mice (Fig. 1*C*, segments defined in Methods). The increased fluid absorption under basal conditions in the ileum but not jejunum of NHERF2 KO mice was confirmed in these experiments (Fig. 1*C*).

NHE3 mRNA expression throughout the intestine was not changed by NHERF2 ablation

No difference was seen in the NHE3 mRNA levels between NHERF2-deficient and WT mice in any of the intestinal segments studied (Fig. 2*A*). We normalized NHE3 mRNA expression to villin, which is a structural BBM component with a similar expression pattern to NHE3, and to RPS9, which is an indicator of overall RNA content, but has the

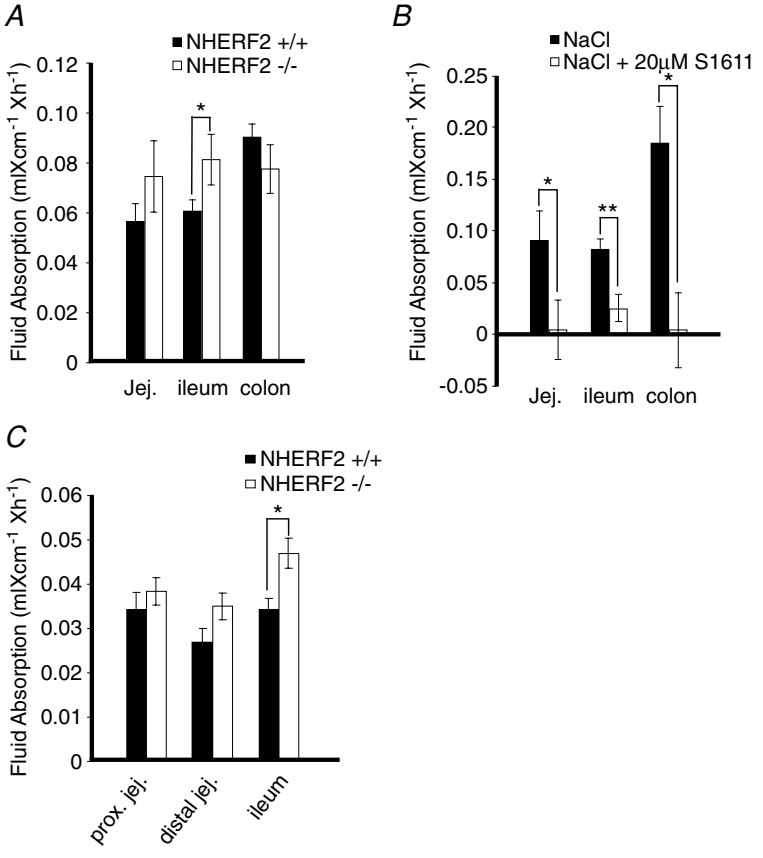

Figure 1. *in vivo* fluid absorption in jejunum, mid ileum and colon of NHERF2-deficient and WT mice
A, no significant differences were observed in fluid absorptive rates in jejunum and colon of NHERF2-deficient mice and WT littermates except in the ileum, in which the fluid absorptive rate was significantly higher in the NHERF2-deficient mice. *B*, 20 μM of S1611, which inhibits NHE3, strongly reduced fluid absorptive rates in all intestinal segments of FVB/N mice, demonstrating that fluid absorptive rates adequately reflect NHE3 activity *in vivo*. *C*, simultaneous fluid absorption measurements in ligated loops of proximal and distal jejunum and ileum of NHERF2-deficient and WT mice. The bars indicate the fluid absorption in NHERF2-deficient and WT ligated loops from different parts of the intestine in the basal state. Basal absorptive rate was similar or higher in the NHERF2-deficient intestine (significant increase in ileum). $n = 6$–9. $^*P < 0.05$, $^{**}P < 0.01$.

disadvantage that changes in a non-epithelial component of the intestine may skew the results.

NHE3 protein in the BBM was not different in NHERF2 KO and WT small intestine

Because the increase in fluid absorptive rates in the ileum of NHERF2-deficient mice was not explained by an increase in the NHE3 mRNA expression, we isolated the BBM from the small intestine of NHERF2 KO and WT mice, and quantified NHE3 BBM protein content in relation to the structural brush border membrane protein villin. Supplementary Fig. 1 demonstrates the experiment from three pooled NHERF2 WT and KO small intestines, where assessment of enrichment against villin is outlined. Figure 2*B* shows four individual preparations from four matched pairs of WT and KO mouse jejuni and Fig. 2*C* shows the same for ilei. No significant difference was seen between NHE3 BBM content in the jejunal as well as the ileal BBM, although variability was stronger in the ileal samples.

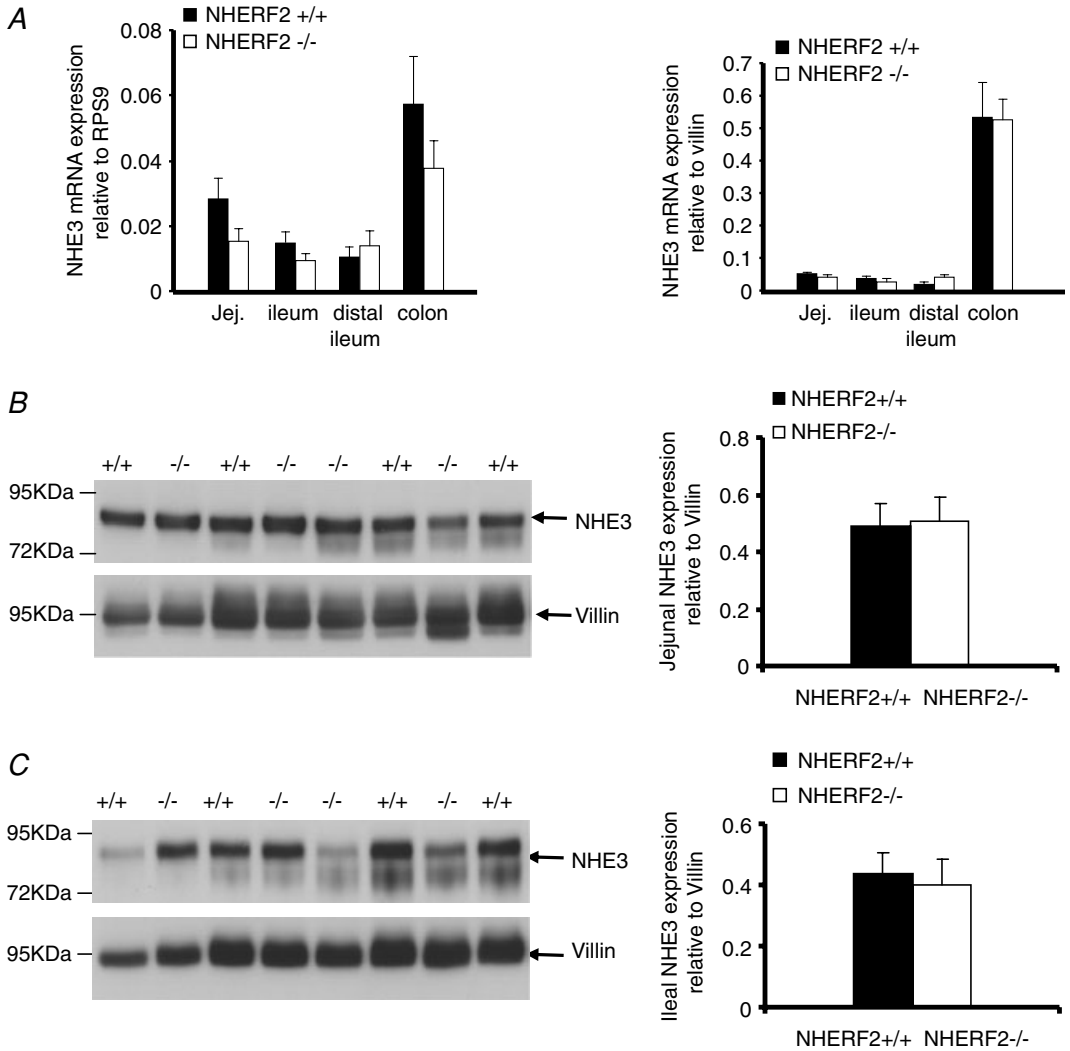

Figure 2. mRNA and protein expression levels of NHE3 in the mucosa of different intestinal segments in NHERF2-deficient mice and WT littermates
A, mRNA expression in scraped mucosa of jejunal (8–10 cm from pylorus), proximal (8–12 cm form ileocaecal junction) and distal (0.5–1 cm from ileocaecal junction) ileal, and colonic mucosa (1 cm distal from the caecocolonic junction to 1 cm proximal to the anus) relative to the ribosomal protein 9 (RPS9), as a control for overall cellular content (left panel), and to the brush border marker gene villin (right panel), which is a expressed in the villus enterocytes. No significant differences were observed in the expression of NHE3 in any intestinal segment. $n = 5$ for each segment and mouse genotype. *B* and *C*, immunoblot and densitometric analysis of scraped jejunal (*B*) and ileal BBM (*C*) for NHE3 content, normalized to the BBM protein villin. No significant difference was observed in small intestinal NHE3 BBM content between NHERF2 KO and WT mice. $n = 4$ for each segment and genotype.

NHERF1/2 mRNA expression throughout the intestine was not changed by NHERF2 ablation

Because basal small intestinal Na^+ or fluid absorptive rates had been found to be reduced in NHERF-1 KO, NHERF1/PDZK1 double KO (Broere *et al.* 2009) and PDZK1-deficient mice, the latter even in the absence of a decreased BBM NHE3 content (Hillesheim *et al.* 2007), we also assessed the mRNA expression levels of the two other NHERF family members, NHERF1 (Fig. 3*A*–*C*, left panel) and PDZK1 (Fig. 3*A*–*C*, right panel), which play a role in agonist-mediated NHE3 inhibition (Yun *et al.* 1997, 1998; Zizak *et al.* 1999; Cinar *et al.* 2007; Zachos *et al.* 2008; Broere *et al.* 2009). NHERF1 mRNA expression was unaltered in all segments; PDZK1 expression on the other hand was significantly reduced in the distal ileum and showed a trend towards lower PDZK1 expression levels in the colon (Fig. 3).

Subcellular NHE3 distribution was altered in NHERF-2 KO mice

Isolated intestinal BBMs contain the microvillar membrane as well as adherent cytoskeletal elements (as they are strongly enriched both for membrane-resident proteins and villin, but to a much lesser extent also for F-actin and the NHERF proteins which associate with

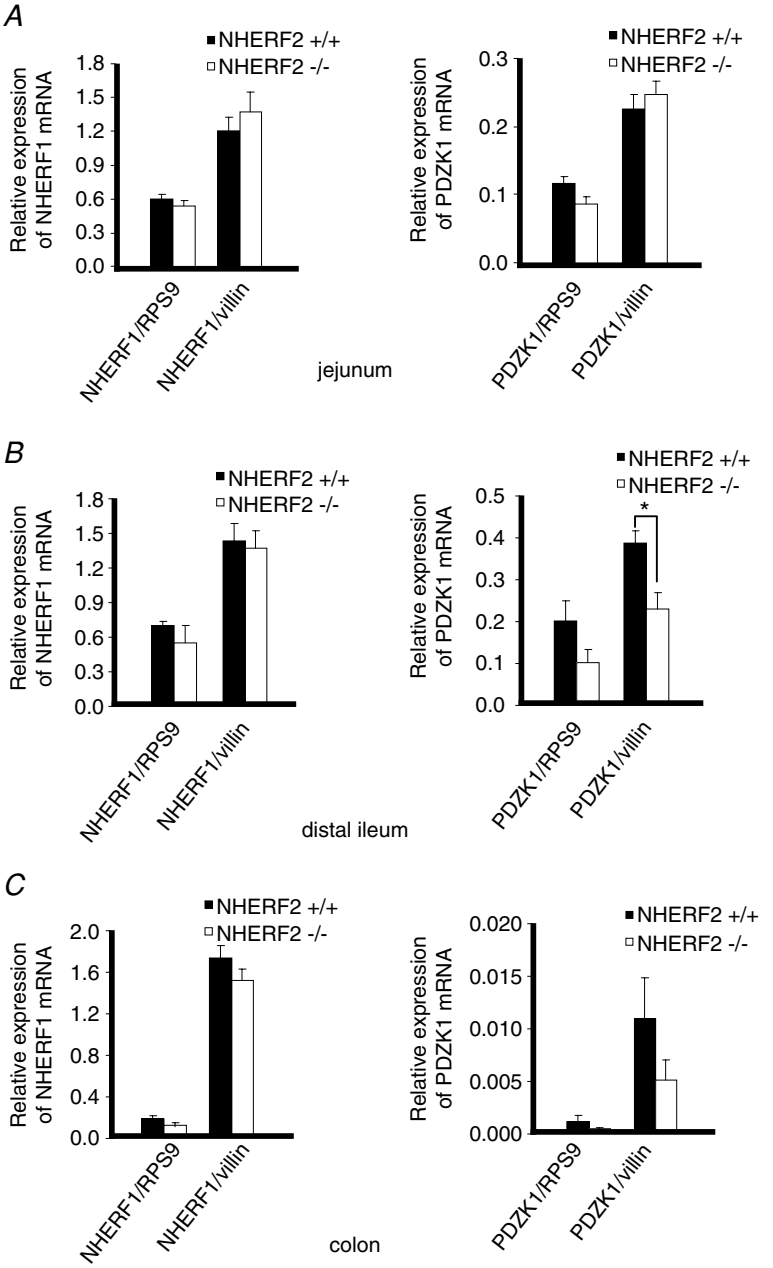

Figure 3. mRNA expression levels of NHERF1 and PDZK1 in jejunal, distal ileal and colonic mucosa in NHERF2-deficient mice and WT littermates
No significant differences were seen in the mRNA expression of two other members of the NHERF family that are involved in NHE3 inhibition in the intestine, except for a trend towards reduced PDZK1 expression in the colon of the NHERF2-deficient mice, and a significantly reduced PDZK1 expression in the distal ileum when standardized against villin. $n = 4$–6. The left panels show the mRNA expression levels for NHERF1 relative to RPS9 and villin; the right panels show the mRNA expression of PDZK1. $^*P < 0.05$.

membrane transporters but are not membrane-resident proteins). Since a different location of NHE3 along the proximal tubule BBM has recently beeen implicated with different transport activity (Riquier *et al.* 2009, 2010), we analysed the distribution of NHE3 along the microvillar axis in jejunum, mid- and distal-ileum, and colon in NHERF2 KO and WT littermates (Fig. 4 and Supplementary Fig. 3 display method). The 'terminal web' region was defined as the region towards the innermost part of the BBM, where the actin signal is particularly strong and which does not stain with the nutrient absorptive transporter PEPT1 (Chen *et al.* 2010). In the jejunum, approximately two-thirds of the overall NHE3 immunoreactivity was in the 'microvillar tip' (upper half of the microvilli) region (Figs 4 and 5, upper panels), whereas in the mid-ileum, approximately two-thirds of NHE3 was in the terminal web region (not shown). In the distal ileum, NHE3 was very strongly terminal web located (Figs 4 and 5, middle panels), and in the colon, NHE3 was predominantly in the microvilli (Figs 4 and 5). There was a tendency for more microvillar NHE3 in all parts of the NHERF2 KO small intestine, but the effect was stronger in the ileum, and particularly strong in distal ileum (Figs 4*B* and 5, middle panels), i.e. in the areas with more NHE3 in the terminal web region in the WT mice. Since a microvillar location of NHE3 appears to be associated with more NHE3 transport function (Fig. 6, and Riquier *et al.* 2010), the higher fluid absorptive rate in the ileum of NHERF2 KO compared to WT mice (Fig. 1*A* and *C*) may be explained by the higher percentage of NHE3 in the microvillar region in these mice. However, given the short segment of intestine that is affected, this is not likely to result in major differences in overall intestinal fluid transport in these mice.

No significant effect of NHERF2 ablation on acid-activated NHE3 activity in the different intestinal segments

The ammonium-prepulse technique was applied to measure acid-activated Hoe642-insensitive Na^+/H^+ exchange activity in BCECF-loaded colonic crypts or microdissected jejunal and ileal villi. The specificity of this technique for assessing acid-activated NHE3 activity has previously been described for colonic crypts (Cinar *et al.* 2007), and was even better for jejunal and ileal villi, as demonstrated by a near-total absence of acid-activated Hoe642-insensitive proton extrusion rate in NHE3-deficient jejunal and ileal enterocytes (Fig. 6*A* and *B*). In addition, 20 μM of the NHE3 inhibitor S1611 strongly inhibited acid-activated Hoe642-insensitive proton flux rates in small intestinal enterocytes (Fig. 6*A* and *B*). Similar experiments have been performed for the colon (Fig. 6*D*).

Acid-activated NHE3 activity varied significantly in the different segments of the WT small intestine, with much lower rates in the distal than the proximal ileum and the jejunum, despite identical conditions for the measurement technique and particular care to acidify enterocytes to a similarly low pH_i (Fig. 6*A*–*C*). The NHE3

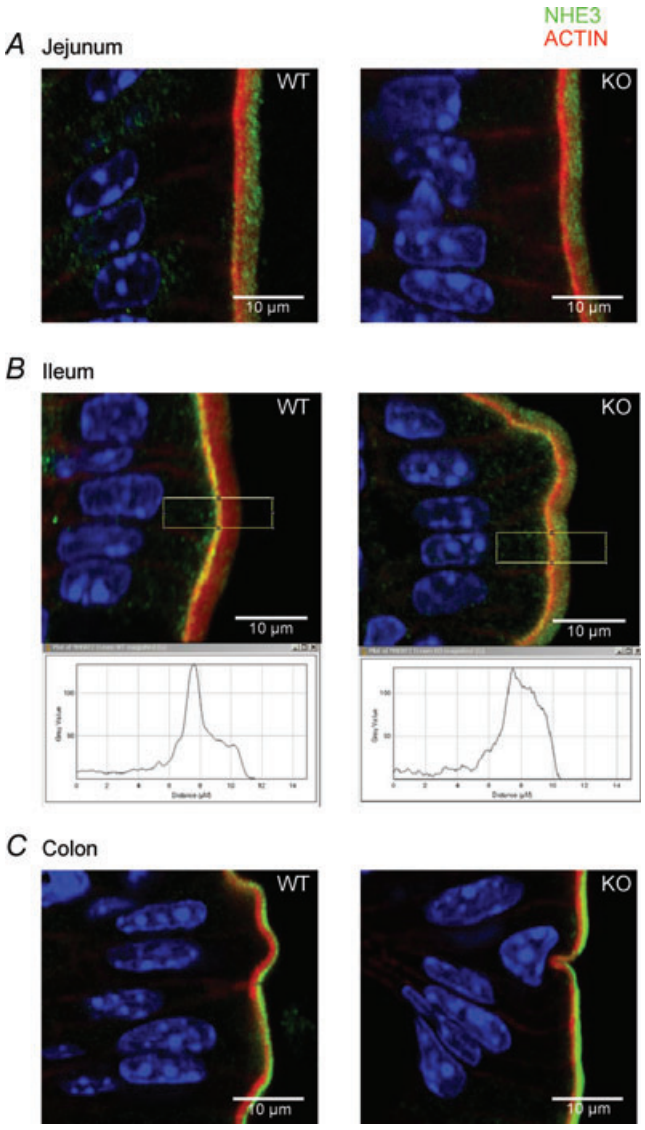

Figure 4. NHE3 subcellular distribution near the brush border membrane
Confocal section through the BBM of WT and NHERF2-deficient mice in jejunal enterocytes (*A*), distal ileal enterocytes (*B*), and colonocytes (*C*), with the apical F-actin cytoskeleton stained red and NHE3 stained green. To assess the relative distribution of NHE3 along the terminal web/microvillar axis, we measured the fluorescence distribution in a chosen area perpendicular to the BBM, which creates one distribution plot as shown in *B*. Five representative areas were selected from BBM of each segment of 3 WT and NHERF2-deficient mice. The fluorescence signal in the terminal web region was set to 1 for each of the 15 curves created for each segment, and relative distribution curves were created for F-actin and for NHE3 (see Fig. 5*B*, and Supplemental Material). Scale bars 10 μm.

activity rates from the colonic crypts are not directly comparable to those obtained from the small intestine, because the acidification protocol is different, and because NHE3 activity is assessed in the enterocytes of the cryptal openings rather than in the very strongly NHE3 expressing surface enterocytes, which are lost during crypt isolation.

No significant differences were observed in NHE3 activity between NHERF2-deficient and WT enterocytes in any intestinal segment (Fig. 6*A*–*D*).

cAMP-induced inhibition of NHE3 activity does not require the presence of NHERF2 in murine jejunum, ileum and colon

NHERF2 coexpression conferred PKA inhibition of NHE3 in PS120 fibroblasts (Lamprecht *et al.* 1998; Zizak *et al.* 1999). We therefore assessed the inhibition of acid-activated NHE3 activity by 10^{-5} M forskolin in different intestinal segments in NHERF2-deficient and WT mice. Forskolin application resulted in a similar degree of NHE3 inhibition in NHERF2-deficient and WT proximal ileum (Fig. 7*A*). Similar results were obtained in the colonocytes in the cryptal openings of isolated colonic crypts (Fig. 7*B*). The inhibitory effect of 10^{-5} M forskolin on the percentage of acid-activated NHE3 activity in the jejunum was not different from that found in the proximal ileum both for NHERF2 KO and WT mice, but we did not repeat the experiments in this segment often enough for full statistical analysis.

Recent data obtained in proximal tubules suggested that NHE3 location in the villus cleft region is associated with reduced function (Riquier *et al.* 2009, 2010). Because we observed that NHE3 in the distal ileum is predominantly localized in a similar region (which we called the 'terminal web' region because it contains the highest amount

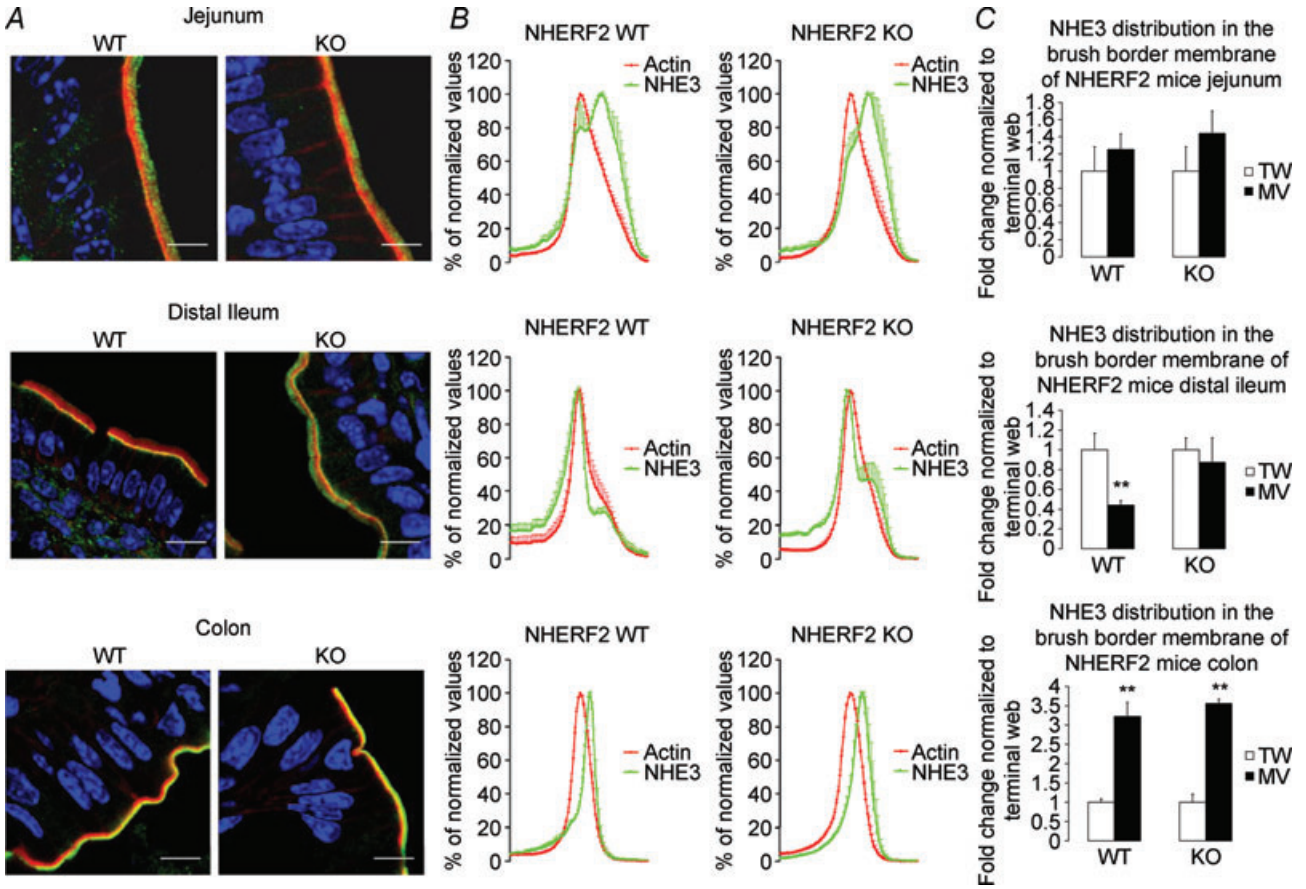

Figure 5. NHERF2 influences the NHE3 distribution in the ileal BBM
A, lower magnification of confocal sections through the BBM of WT and NHERF2-deficient mice in jejunal enterocytes, distal ileal enterocytes, and colonocytes. *B*, relative distribution curves of F-actin and NHE3 along the BBM in jejunum, distal ileum and colon of WT and NHERF2-deficient mice. *C*, bar graphs representing the amount of NHE3 that is terminal web/intravillar cleft associated and the microvillus tip (upper part of the microvilli) associated for each of the studied segments. An exact method description is found in the Supplemental Material. It is evident that NHE3 distribution varies, with a predominant microvillar distribution in jejunum and colon, and predominant terminal web localization in the distal ileum. $n = 3$ for each segment and genotype. The scale bars represent 10 μm.

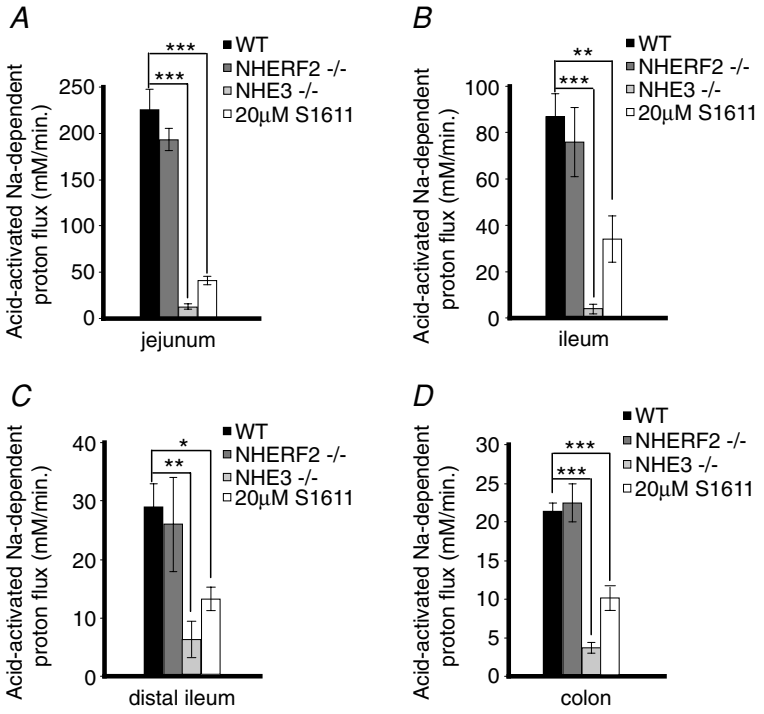

Figure 6. Effect of NHERF2 ablation on acid-activated NHE3 activity in the different intestinal segments
A–C, fluorometrically determined acid-activated NHE3 transport rates in the different segments of WT, NHERF2-deficient, NHE3-deficient and S1611-treated jejunal (*A*), mid-ileal (approx 4–6 cm proximal to the ileocaecal valve) (*B*), and distal ileal (last 1 cm before ileocaecal valve) (*C*) villi. *D*, NHE3 activity in the cryptal mouth of isolated colonic crypts of WT, NHERF2-, and NHE3-deficient and S1611-treated mice. Whereas no significant differences were observed in acid-activated NHE3 activity between WT and NHERF2 mice in jejunum, ileum and colon, there was a strikingly low acid-activated NHE3 activity in the distal ileum (*C*), which correlates with the predominant terminal web localization of NHE3 in this intestinal segment. *D*, NHE3 activity measurements in colonic crypts follow a different experimental protocol (see Methods and text) and can therefore not be compared directly with NHE3 activity measurements in small intestinal villi, but no difference in acid-activated NHE3 activity was observed between NHERF2-deficient and WT crypts. $n = 4–7$, $^{*}P < 0.05$, $^{**}P < 0.01$, $^{***}P < 0.001$.

of actin) (Figs 4 and 5), we also studied the effect of forskolin on acid-activated NHE3 activity in the very distal ileum. Interestingly, the distal ileum showed not only a strongly reduced acid-activated NHE3 activity, but also a low (non-significant) inhibitory effect of forskolin in the WT enterocytes (Fig. 7*A*). Likewise, no significant FSK inhibition was observed in the NHERF2 KO mice (Fig. 7*A*).

$[Ca^{2+}]_i$-induced NHE3 inhibition requires NHERF2 expression

In NHE3-expressing fibroblasts, $[Ca^{2+}]_i$-dependent NHE3 inhibition requires the expression of NHERF2 (Kim *et al.* 2002; Lee-Kwon *et al.* 2003). To investigate the role of NHERF2 in $[Ca^{2+}]_i$-induced inhibition of NHE3 activity in murine small and large intestine,

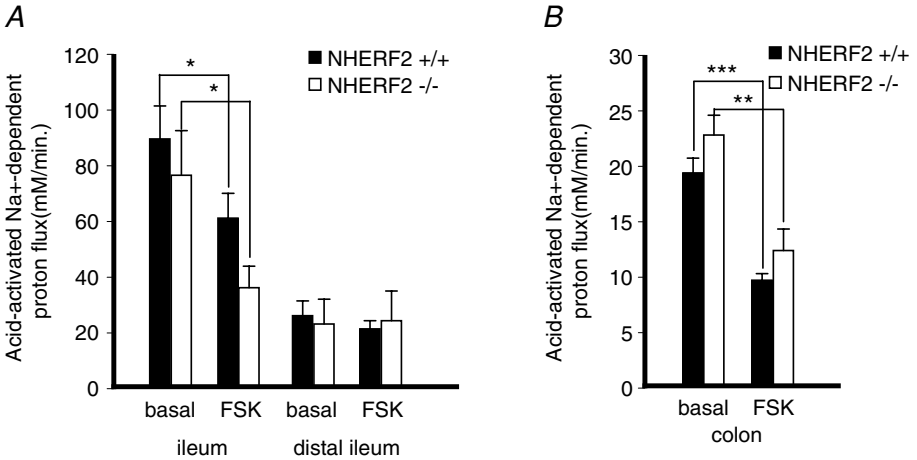

Figure 7. cAMP-induced inhibition of acid-activated NHE3 activity in NHERF2-deficient and WT ileum (*A*) and in colonic crypts (*B*)
Forskolin (10^{-5} M)-mediated inhibition of acid-activated NHE3 activity in the mid (5 cm from ileocaecal junction) and the distal ileum (last cm before ileocaecal junction) of NHERF2 deficient and WT mice (*A*). No difference in the inhibitory effect of forskolin was seen in the mid ileum (*A*) or the colon (*B*). Forskolin inhibition in the distal ileum, which was weak in WT, was not observed in NHERF2-deficient terminal ileum. $n = 4–8$, $^{*}P < 0.05$,$^{**}P < 0.01$, $^{***}P < 0.001$.

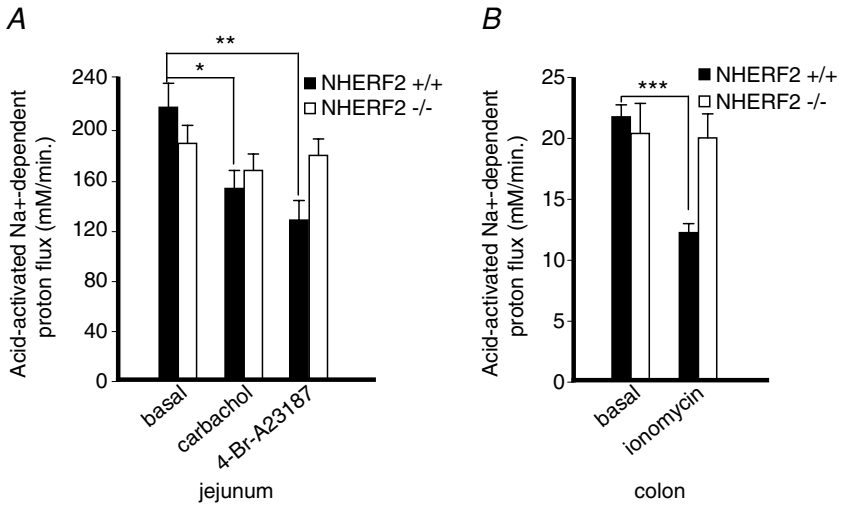

Figure 8. Ca^{2+}-induced NHE3 inhibition requires NHERF2 expression
A, both carbachol (10^{-3} M) and the Ca^{2+}ionophore 4-BrA23187 inhibited acid-activated NHE3 activity in WT, but were without significant inhibitory effect in NHERF2-deficient jejunal villi. *B*, the same requirement for NHERF2 expression was found in colonic crypts, where 2 μM of the Ca^{2+}-ionophore ionomycin was applied 3 min before adding back Na^+. Thus, both receptor-dependent and -independent Ca^{2+}-mediated NHE3 inhibition was abolished in the absence of NHERF-2 expression in small and large intestine. $n = 4$–9, $^*P < 0.05$, $^{**}P < 0.01$, $^{***}P < 0.001$.

we applied 10^{-3} M carbachol or 20 μM 4-Br-A23187 5 min before Na^+-dependent recovery to microdissected, BCECF-loaded jejunal NHERF2-deficient and WT villi. The jejunum was chosen for these experiments because carbachol elicited consistent inhibition of acid-activated NHE3 activity in the villi of this intestinal segment of WT mice. Carbachol and 4-Br-A23187 inhibited NHE3 activity in WT but not in NHERF2-deficient jejunal villi (Fig. 8*A*). Similar experiments were performed in BCECF-loaded colonic crypts, using preincubation with 2 mM ionomycin for 2 min (as described in the experiments with NHE3-expressing PS120 cells, Kim *et al.* 2002) (Fig. 8*B*), which resulted in significant inhibition of acid-activated NHE3 activity in WT but not NHERF2 KO colonic crypts. This indicates that NHERF2 plays a major role in $[Ca^{2+}]_i$-dependent NHE3 inhibition.

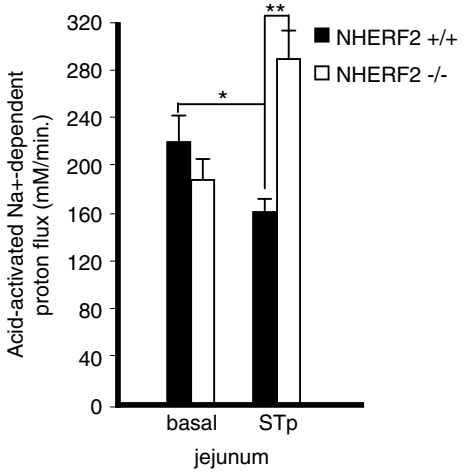

Figure 9. cGMP-dependent inhibition of NHE3 activity requires NHERF2 expression in jejunum
Application 10^{-7} M of the *Escherichia coli* heat stable toxin peptide (STp) approx. 5 min before Na^+ re-addition significantly inhibited acid-activated NHE3 activity in WT jejunal villi, whereas STp even increased acid-activated NHE3 activity in NHERF2-deficient villi. $n = 4$–7, $^*P < 0.05$, $^{**}P < 0.01^{***}P < 0.001$.

cGMP-dependent inhibition of NHE3 activity requires NHERF2 in murine jejunum

Escherichia coli heat-stable enterotoxin (STp) binds to guanylate cyclase-C in the luminal enterocyte membrane and increases intracellular cGMP levels (Vaandrager *et al.* 1993). STp at 10^{-7} M induced inhibition of acid-activated NHE3 activity in WT jejunal villi, whereas an increase of NHE3 activity after STp treatment was observed in the NHERF2 KO jejunal villi (Fig. 9). The effect of STa (these experiments were done with STa when it was still available from Sigma) on acid-activated NHE3 activity had also been studied in isolated colonic crypts, but no significant inhibition of NHE3 activity was seen, possibly because STa could not access its luminal receptors in this preparation (data not shown).

The reason for the increase in NHE3 activity after STp application in the NHERF2-deficient small intestinal villi is at present unknown. However, the data unequivocally demonstrate that NHERF2 is necessary for cGMP-mediated inhibition of NHE3 activity in the small intestine.

Discussion

The goal of the current study was to examine NHE3 expression, membrane localization, and in particular, agonist-mediated NHE3 transport regulation in different intestinal segments of NHERF2-deficient mice and WT littermates.

The first finding was an unexpected increase in the basal fluid absorption rates in the ileum of anaesthetized

NHERF-2 deficient mice compared to WT littermates, and no significant difference in fluid absorption in the other studied intestinal segments. In search of an explanation we observed (1) no difference in NHE3 mRNA expression levels, (2) no difference in NHE3 protein content in isolated BBM vesicles (which contain the complete BBM plus subapical cytoskeletal structures), but (3) significant differences in the relative distribution of NHE3 in the microvillar tip region *versus* the terminal web region along the small intestine of WT mice. NHE3 was found in a predominantly microvillar location in the proximal jejunum, and a gradual shift toward a higher percentage of terminal web NHE3 in the ileum was observed. A relatively higher percentage of NHE3 in the microvilli was associated with higher NHE3 transport rates within the different small intestinal segments (Fig. 6). NHERF2 deficiency affected this distribution, in that a more diffuse distribution with more NHE3 in the microvilli was observed in the ileum of NHERF2-deficient mice. This may explain the higher fluid absorption rates in the NHERF2 KO ileum. In the proximal tubule, NHE3 transport activity has recently been demonstrated to be regulated by trafficking from the intervillar clefts into the microvilli (Riquier *et al.* 2009, 2010). Movement of NHE3 from the tip of the microvilli to the intervillar cleft was associated with reduced transport activity. This observation resembles somewhat that seen in the murine ileum. However, we believe that a part of the ileal NHE3 was likely to have been localized in recycling endosomes in the terminal web rather than the microvillar base, because most NHE3-mediated immunofluorescence could be assessed at the innermost part of the F-actin band. Danielsen & Hansen (2003) describe apical membrane invaginations or 'deep apical tubules' that extend up to 0.5–1 μm into the underlying terminal web region in small intestinal brush border, so we cannot differentiate between a recycling endosome or this deep apical tubule localization of NHE3. However, this localization was associated with reduced acid-activated NHE3 activity and an almost complete loss of inhibition by forskolin, resembling the situation in the kidney. Accepting the concept that a microvillar tip location of NHE3 correlates with higher NHE3 transport rates, the increased fluid absorptive rates in the distal ileum of NHERF2 KO mice may be explained by the finding of a higher percentage of overall NHE3 in the microvillar tip compared to the terminal web region. These findings are the first hint that NHERF2 is somehow involved in membrane tethering of NHE3 within a specific region of the intestinal microvilli. An endogenous NHE3 inhibitor may keep NHE3 in the 'terminal web' location in the anaesthetized mice in a NHERF2-dependent fashion, and this 'endogenous inhibition' may be absent or reduced in the NHERF2 KO ileum.

The next goal of this study was therefore to assess the importance of NHERF2 expression for agonist-mediated NHE3 inhibition in the murine intestine. PS120/NHE3V cells require the expression of NHERF2 or NHERF1 for inhibition of NHE3 by cAMP analogues (Zizak *et al.* 1999). Likewise, the PKA-induced, CFTR-mediated inhibition of NHE3 in the *Xenopus* A9 cells required NHERF2 expression (Bagorda *et al.* 2002). However, NHERF1 was previously found to be important for PKA-mediated NHE3 inhibition in the kidney, but not in the intestine (Weinman *et al.* 2003, 2005; Murtazina *et al.* 2007; Broere *et al.* 2009), demonstrating the cell-specificity of NHERF1-mediated NHE3 regulation. Likewise, NHERF2 expression appeared not to be necessary for cAMP-mediated inhibition of NHE3 in any of the segments of the murine intestine except possibly the distal ileum. The latter segment is characterized by a low NHE3 activity, strongly reduced inhibitor action of forskolin (even in the WT mice), and a predominant terminal web/intervillar cleft localization of NHE3. It is possible that endogenous factors inhibit NHE3 in this narrow part of the murine gut to prevent blockage by mucus/luminal contents (with a possible role of NHERF2 in this endogenous inhibition; see above). However, this suggested that this segment of the gut is not optimal to study the molecular regulation of inhibitory NHE3 signals.

Interestingly, forskolin-induced inhibition of NHE3 in the jejunum or proximal ileum was rapid (we added forskolin only 2 min prior to re-addition of Na^+) and was not associated with a detectable retrieval of NHE3 from its microvillar location up to 20 min after forskolin application in either WT or NHERF2-deficient jejunum (data not shown). This is in concordance with studies in PS120/NHE3/NHERF1 or NHERF2 cells, where no change in membrane abundance of NHE3 was seen despite transport inhibition by cAMP (Lamprecht *et al.* 1998).

Consistent with the findings in heterologous expression systems, NHERF2 ablation abolished both receptor-dependent and receptor-independent Ca^{2+}-mediated NHE3 inhibition in both murine small intestine and colon. We could not, however, detect a carbachol-induced change of NHE3 membrane localization (e.g. retrieval to the terminal web or complete exocytosis from the membrane), as was the predicted mechanism for Ca^{2+}-mediated NHE3 inhibition in heterologous expression systems (Kim *et al.* 2002). Even at concentrations sufficient for full muscarinic receptor activation, carbachol inhibits only a fraction of the acid-activated NHE3 activity that is inhibited by the NHE3 inhibitor S1611. It is therefore possible that the signalling events following muscarinergic receptor activation acts on a subset of BBM-resident NHE3 only. It is a challenge for the future to characterize such subpools of NHE3 and find out what may determine the agonist targeting of such subpools of NHE3. The first steps toward delineation of different pools of NHE3 are under way (Alexander *et al.* 2005; Alexander & Grinstein, 2009).

Ca^{2+}-mediated NHE3 inhibition was also abolished in the PDZK1 deficient murine colon (Cinar *et al.* 2007), and in NHE3-expressing Caco-2bbe cells after siRNA-mediated PDZK1 silencing (Zachos *et al.* 2009). Zachos *et al.* (2009) searched for the molecular role of PDZK1 in Ca^{2+}-mediated NHE3 inhibition and observed strongly reduced NHE3 membrane abundance in Caco-2bbe cells after PDZK1 silencing. In the PDZK1-deficient colon, NHE3 membrane abundance was normal but NHE3 mRNA was strongly increased, suggesting that increased production may compensate for the reduced membrane retention time (Cinar *et al.* 2007). We therefore wondered if, similar to the results in PDZK1-deficient mice, NHE3 mRNA or expression of the other NHE3-inhibitory PDZ-adaptor proteins was altered in the NHERF2-deficient intestine. No significant change in mRNA expression for NHE3, NHERF1 or PDZK1 was found, except the small reduction of PDZK1 mRNA when normalized to villin in the distal ileum, whose significance is uncertain at present. Thus, it appears that both NHERF2 and PDZK1 are required for Ca^{2+}-mediated NHE3 inhibition, but that the two proteins have different molecular tasks in this process, explaining that both proteins cannot substitute for each other and both are essential.

The guanylins and their bacterial analogue heat-stable *Eschericha coli* enterotoxin (STa or STp) inhibit NHE3 via an intracellular cGMP increase (Donowitz *et al.* 2005). Vaandrager *et al.* (2000) provided evidence that whereas cGMP inhibits salt absorption in both the small and the large intestine, the involved signalling pathways are different. In the small intestine, but not the colon, expression of the cGMP-dependent protein kinase II is necessary for inhibition of NHE3 by STa, whereas in the colon, cGMP-mediated inhibition of cAMP-specific phosphodiesterases may result in an increase in PKA activity, which also results in NHE3 inhibition. Cha *et al.* (2005) provided biochemical evidence for a binding of NHERF2, but not NHERF1, to cGKII, and only a coexpression of both NHERF2 and cGKII with NHE3 in PS120 cells resulted in NHE3 inhibition by cGMP analogues. Thus, the lack of inhibition of NHE3 by the heat-stable *E.coli* toxin peptide STp in the small intestine in the absence of NHERF2 agrees well with the data from the heterologous expression system. What was totally surprising, however, was the significant stimulation of NHE3 activity by STp in NHERF2-deficient small intestinal villi. It is known that STp stimulates enterocyte cGMP production via binding to the transmembrane receptor enzyme guanylate cyclase-C (GCC) (Vaandrager, 2002), which is expressed not only in the crypt but also in the villus enterocyte apical membrane and therefore in part shows a similar cellular distribution to NHE3 (Swenson *et al.* 1996). Using the C-terminus of the GCC as bait in yeast two-hybrid screening, Scott *et al.* (2002) identified a PDZ protein of the NHERF family, which is now called NHERF4 (Thelin *et al.* 2005). NHERF4 also binds to NHE3 but stimulates its activity in a Ca^{2+}-dependent fashion when co-expressed with NHE3 in PS120 cells (Zachos *et al.* 2008). It is possible, but as yet speculative, that in the absence of NHERF2, the NHERF4 clusters to GCC upon STp binding and activates NHE3. In any case the findings do underline how crucial each member of the NHERF family is for receptor-mediated regulation of ion transporters, similar to what we found earlier for CFTR regulation (Singh *et al.* 2009).

In summary, our study demonstrates that the expression of the PDZ-adaptor NHERF2 plays a highly selective, signal- and segment-specific role in NHE3 activity regulation in the intestine. A major function of intestinal NHERF2 may lie in conferring inhibitory (as well as stimulatory, Lin *et al.* 2010) signals to NHE3. A loss of Ca^{2+}-mediated NHE3 inhibition may confer increased resistence to rotavirus enterotoxins (Morris *et al.* 1999; Lorrot & Vasseur, 2007) as well as enterotoxin-released neurotransmittors such as serotonin (Lundgren *et al.* 2002; Gershon & Tack, 2007; Xue *et al.* 2007), or to ATP released from the cells during stress (Xue *et al.* 2007). A loss of STa-mediated inhibition may increase intestinal resistance to the most common form of traveller's diarrhoea (Fleckenstein *et al.* 2010). In addition to its prominent role in agonist regulation of NHE3, NHERF2 appears to be involved in the tethering of NHE3 to the terminal web/intravillar cleft region and releasing it from this location in an agonist-specific fashion. We could only study this phenomenon in the ileum, because that was the only segment that displayed a NHERF2-dependent segregation of NHE3 towards the terminal web region (this paper, and Lin *et al.* 2010). However, a recent publication confirmed this function of NHERF2 in heterologous expression models (Cha *et al.* 2010). While more work is needed to understand the concerted action of several members of the NHERF family in agonist-specific NHE3 regulation, it has become clear that NHERF2 may be a major player in NHE3 regulation as well as an interesting drug target in diarrhoeal diseases.

References

Alexander RT, Furuya W, Szászi K, Orlowski J & Grinstein S (2005). Rho GTPases dictate the mobility of the Na/H exchanger NHE3 in epithelia: role in apical retention and targeting. *Proc Natl Acad Sci U S A* **102**, 12253–12258.

Alexander RT & Grinstein S (2009). Tethering, recycling and activation of the epithelial sodium-proton exchanger, NHE3. *J Exp Biol* **212**, 1630–1637.

Bachmann O, Wüchner K, Rossmann H, Leipziger J, Osikowska B, Colledge WH, Ratcliff R, Evans MJ, Gregor M & Seidler U (2003). Expression and regulation of the Na^+-K^+-$2Cl^-$ cotransporter NKCC1 in the normal and CFTR-deficient murine colon. *J Physiol* **549**, 525–536.

Bachmann O, Riederer B, Rossmann H *et al.* (2004). The Na^+/H^+ exchanger isoform 2 is the predominant NHE isoform in murine colonic crypts and its lack causes NHE3 upregulation. *Am J Physiol Gastrointest Liver Physiol* **287**, G125–133.

Bagorda A, Guerra L, Di Sole F, Hemle-Kolb C, Cardone RA, Fanelli T, Reshkin SJ, Gisler SM, Murer H & Casavola V (2002). Reciprocal protein kinase A regulatory interactions between cystic fibrosis transmembrane conductance regulator and Na^+/H^+ exchanger isoform 3 in a renal polarized epithelial cell model. *J Biol Chem* **277**, 21480–21488.

Broere N, Hillesheim J, Tuo B, Jorna H, Houtsmuller AB, Shenolikar S, Weinman EJ, Donowitz M, Seidler U, de Jonge HR & Hogema BM (2007). Cystic fibrosis transmembrane conductance regulator activation is reduced in the small intestine of Na^+/H^+ exchanger 3 regulatory factor 1 (NHERF-1)- but not NHERF-2-deficient mice. *J Biol Chem* **282**, 37575–37584.

Broere N, Chen M, Cinar A, Singh AK, Hillesheim J, Riederer B, Lünnemann M, Rottinghaus I, Krabbenhöft A, Engelhardt R, Rausch B, Weinman EJ, Donowitz M, Hubbard A, Kocher O, de Jonge HR, Hogema BM & Seidler U (2009). Defective jejunal and colonic salt absorption and altered Na^+/H^+ exchanger 3 (NHE3) activity in NHE regulatory factor 1 (NHERF1) adaptor protein-deficient mice. *Pflugers Arch* **457**, 1079–1091.

Cha B, Kim JH, Hut H, Hogema BM, Nadarja J, Zizak M, Cavet M, Lee-Kwon W, Lohmann SM, Smolenski A, Tse CM, Yun C, de Jonge HR & Donowitz M (2005). cGMP inhibition of Na^+/H^+ antiporter 3 (NHE3) requires PDZ domain adapter NHERF2, a broad specificity protein kinase G-anchoring protein. *J Biol Chem* **280**, 16642–16650.

Cha B, Zhu XC, Chen W, Jones M, Ryoo S, Zachos NC, Chen TE, Lin R, Sarker R, Kenworthy AK, Tse M, Kovbasnjuk O & Donowitz M (2010). NHE3 mobility in brush borders increases upon NHERF2-dependent stimulation by lyophosphatidic acid. *J Cell Sci* **123**, 2434–2443.

Chen M, Singh AK, Xiao F, Dringenberg U, Wang J, Engelhardt R, Yeruva S, Rubio-Aliaga I, Näßl AM, Kottra G, Daniel H & Seidler UE (2010). Gene ablation for PEPT1 in mice abolishes the effects of dipeptides on small intestinal fluid absorption, short circuit current and intracellular pH. *Am J Physiol Gastrointest Liver Physiol* **299**, G265–274.

Cinar A, Chen M, Riederer B, Bachmann O, Wiemann M, Manns M, Kocher O & Seidler U (2007). NHE3 inhibition by cAMP and Ca^{2+} is abolished in PDZ-domain protein PDZK1-deficient murine enterocytes. *J Physiol* **581**, 1235–1246.

Danielsen EM & Hansen GH (2003). Lipid rafts in epithelial brush borders: atypical membrane microdomains with specialized functions. *Biochim Biophys Acta* **1617**, 1–9.

Donowitz M, Cha B, Zachos NC, Brett CL, Sharma A, Tse CM & Li X (2005). NHERF family and NHE3 regulation. *J Physiol* **567**, 3–11.

Fleckenstein JM, Hardwidge PR, Munson GP, Rasko DA, Sommerfelt H & Steinsland H (2010). Molecualr mechanisms of enterotoxigenic *Escherichia coli* infection. *Microbes Infect* **12**, 89–98.

Gershon MD & Tack J (2007). The serotonin signaling system: from basic understanding to drug development for functional GI disorders. *Gastroenterology* **132**, 397–414.

Hall RA, Ostedgaard LS, Premont RT, Blitzer JT, Rahman N, Welsh MJ & Lefkowitz RJ (1998). A C-terminal motif found in the β2-adrenergic receptor, P2Y1 receptor and cystic fibrosis transmembrane conductance regulator determines binding to the Na^+/H^+ exchanger regulatory factor family of PDZ proteins. *Proc Natl Acad Sci U S A* **95**, 8496–8501.

Hansen GH, Rasmussen K, Niels-Christiansen LL & Danielsen EM (2009). Endocytic trafficking from the small intestinal brush border probed with FM dye. *Am J Physiol Gastrointest Liver Physiol* **297**, G708–G715.

Hegyi P, Rakonczay Z Jr, Gray MA & Argent BE (2004). Measurement of intracellular pH in pancreatic duct cells: a new method for calibrating the fluorescence data. *Pancreas* **28**, 427–434.

Hillesheim J, Riederer B, Tuo B, Chen M, Manns M, Biber J, Yun C, Kocher O & Seidler U (2007). Down regulation of small intestinal ion transport in PDZK1-(CAP70/NHERF3) deficient mice. *Pflugers Arch* **454**, 575–586.

Hirokawa N, Tilney L, Fujiwara K & Heuser JE (1982). Organization of actin, myosin and intermediate filaments in the brush border membrane of intestinal epithelial cells. *J Cell Biol* **94**, 425–443.

Kim JH, Lee-Kwon W, Park JB, Ryu SH, Yun CH & Donowitz M (2002). Ca^{2+}-dependent inhibition of Na^+/H^+ exchanger 3 (NHE3) requires an NHE3-E3KARP-α-actinin-4 complex for oligomerization and endocytosis. *J Biol Chem* **277**, 23714–23724.

Lamprecht G, Weinman EJ & Yun CH (1998). The role of NHERF and E3KARP in the cAMP-mediated inhibition of NHE3. *J Biol Chem* **273**, 29972–29978.

Lee-Kwon W, Kawano K, Choi JW, Kim JH & Donowitz M (2003). Lysophosphatidic acid stimulates brush border Na^+/H^+ exchanger 3 (NHE3) activity by increasing its exocytosis by an NHE3 kinase A regulatory protein-dependent mechanism. *J Biol Chem* **278**, 16494–16501.

Lin S, Yeruva S, He P, Singh AK, Zhang H, Chen M, Lamprecht G, de Jonge HR, Tse M, Donowitz M, Hogema BM, Chun J, Seidler U & Yun CC (2010). Lysophosphatidic acid stimulates the intestinal brush border Na^+/H^+ exchanger 3 and fluid absorption via LPA_5 and NHERF2. *Gastroenterology* **138**, 649–658.

Lorrot M, Vasseur M (2007). How do the rotavirus NSP4 and bacterial enterotoxins lead differently to diarrhea? *Virol J* **4**, 31.

Lundgren O (2002). Enteric nerves and diarrhoea. *Pharmacol Toxicol* **90**, 109–120.

Morris AP, Scott JK, Ball JM, Zeng CQY, O'Neal WK, Estes MK (1999). NSP4 elicits age-dependent diarrhea and Ca^{2+}-mediated I^- influx into intestinal crypts of CF mice. *Am J Physiol Gastrointest Liver Physiol* **277**, G431–444.

Murtazina R, Kovbasnjuk O, Zachos NC, Li X, Chen Y, Hubbard A, Hogema BM, Steplock D, Seidler U, Hoque KM, Tse CM, De Jonge HR, Weinman EJ & Donowitz M (2007). Tissue-specific regulation of sodium/proton exchanger isoform 3 activity in Na^+/H^+ exchanger regulatory factor 1 (NHERF1) null mice. cAMP inhibition is differentially dependent on NHERF1 and exchange protein directly activated by cAMP in ileum versus proximal tubule. *J Biol Chem* **282**, 25141–25151.

Riquier AD, Lee DH & McDonough AA (2009). Renal NHE3 and NaPi2 partition into distinct membrane domains. *Am J Physiol Cell Physiol* **296**, C900–910.

Riquier AD, Leong PK, Pihakaski-Maunsbach K & McDonough AA (2010). Angiotensin II stimulates trafficking of NHE3, NaPi2, and associated proteins into the proximal tubule microvilli. *Am J Physiol Renal Physiol* **298**, F177–186.

Schultheis PJ, Clarke LL, Meneton P, Miller ML, Soleimani M, Gawenis LR, Riddle TM, Duffy JJ, Doetschman T, Wang T, Giebisch G, Aronson PS, Lorenz JN & Shull GE (1998). Renal and intestinal absorptive defects in mice lacking the NHE3 Na^+/H^+ exchanger. *Nat Genet* **19**, 282–285.

Schwark JR, Jansen HW, Lang HJ, Krick W, Burckhardt G & Hropot M (1998). S3226, a novel inhibitor of Na^+/H^+ exchanger subtype 3 in various cell types. *Pflügers Arch* **436**, 797–800.

Scott RO, Thelin WR & Milgram SL (2002). A novel PDZ protein regulates the activity of guanylyl cyclase C, the heat-stable enterotoxin receptor. *J Biol Chem* **277**, 22934–22941.

Singh AK, Riederer B, Krabbenhöft A, Rausch B, Bonhagen J, Lehmann U, de Jonge HR, Donowitz M, Yun C, Weinman EJ, Kocher O, Hogema BM & Seidler U (2009). Differential roles of NHERF1, NHERF2, and PDZK1 in regulating CFTR-mediated intestinal anion secretion in mice. *J Clin Invest* **119**, 540–550.

Singh AK, Riederer B, Chen M, Xiao F, Krabbenhöft A, Engelhardt R, Nylander O, Soleimani M & Seidler UE (2010). The switch of intestinal Slc26 exchangers from anion absorptive to HCO_3^- secretory mode is dependent on CFTR anion channel function. *Am J Physiol Cell Physiol* **298**, C1057–1065.

Swenson ES, Mann EA, Jump ML, Witte DP & Giannella RA (1996). The guanylin/STa receptor is expressed in crypts and apical epithelium throughout the mouse intestine. *Biochem Biophys Res Commun* **225**, 1009–1014.

Thelin WR, Hodson CA & Milgram SL (2005). Beyond the brush border: NHERF4 blazes new NHERF turf. *J Physiol* **567**, 13–19.

Tse CM, Ma AI, Yang VW, Watson AJ, Levine S, Montrose MH, Potter J, Sardet C, Pouyssegur J & Donowitz M (1991). Molecular cloning and expression of a cDNA encoding the rabbit ileal villus cell basolateral membrane Na^+/H^+ exchanger. *EMBO J* **10**, 1957–1967.

Vaandrager AB, Schulz S, De Jonge HR & Garbers DL (1993). Guanylyl cyclase C is an N-linked glycoprotein receptor that accounts for multiple heat-stable enterotoxin-binding proteins in the intestine. *J Biol Chem* **268**, 2174–2179.

Vaandrager AB, Bot AG, Ruth P, Pfeifer A, Hofmann F & De Jonge HR (2000). Differential role of cyclic GMP-dependent protein kinase II in ion transport in murine small intestine and colon. *Gastroenterology* **118**, 108–114.

Vaandrager AB (2002). Structure and function of the heat-stable enterotoxin receptor/guanylyl cyclase C. *Mol Cell Biochem* **230**, 73–83.

Weinman EJ, Steplock D & Shenolikar S (2003). NHERF-1 uniquely transduces the cAMP signals that inhibit sodium-hydrogen exchange in mouse renal apical membranes. *FEBS Lett* **536**, 141–144.

Weinman EJ, Cunningham R, Wade JB & Shenolikar S (2005). The role of NHERF-1 in the regulation of renal proximal tubule sodium-hydrogen exchanger 3 and sodium-dependent phosphate cotransporter 2a. *J Physiol* **567**, 27–32.

Xue J, Askwith C, Javed NH & Cooke HJ (2007). Autonomic nervous system and secretion across the intestinal mucosal surface. *Auton Neurosci* **133**, 55–63.

Yun CH, Oh S, Zizak M, Steplock D, Tsao S, Tse CM, Weinman EJ & Donowitz M (1997). cAMP-mediated inhibition of the epithelial brush border Na^+/H^+ exchanger, NHE3, requires an associated regulatory protein. *Proc Natl Acad Sci U S A* **94**, 3010–3015.

Yun CH, Lamprecht G, Forster DV & Sidor A (1998). NHE3 kinase A regulatory protein E3KARP binds the epithelial brush border Na^+/H^+ exchanger NHE3 and the cytoskeletal protein ezrin. *J Biol Chem* **273**, 25856–25863.

Zachos NC, Tse M & Donowitz M (2005). Molecular physiology of intestinal Na^+/H^+ exchange. *Annu Rev Physiol* **67**, 411–443.

Zachos NC, Hodson C, Kovbasnjuk O, Li X, Thelin WR, Cha B, Milgram S & Donowitz M (2008). Elevated intracellular calcium stimulates NHE3 activity by an IKEPP (NHERF4) dependent mechanism. *Cell Physiol Biochem* **22**, 693–704.

Zachos NC, Li X, Kovbasnjuk O, Hogema B, Sarker R, Lee LJ, Li M, De Jonge H & Donowitz M (2009). NHERF3 (PDZK1) contributes to basal and calcium inhibition of NHE3 activity in Caco-2BBe cells. *J Biol Chem* **284**, 23708–23718.

Zizak M, Lamprecht G, Steplock D, Tariq N, Shenolikar S, Donowitz M, Yun CH & Weinman EJ (1999). cAMP-induced phosphorylation and inhibition of Na^+/H^+ exchanger 3 (NHE3) are dependent on the presence but not the phosphorylation of NHE regulatory factor. *J Biol Chem* **274**, 24753–24758.

Author contributions

Conception and design of the experiments: M.C., A. S., A.C., S.Y., B.R., AK.S, J.L. B.H. and U.S.; collection, analysis and interpretation of data: M.C, A.C., S.Y., B.R., AK.S., J.L., A.S., J.B., B.H., U.S.; drafting the article or revising it critically for important intellectual content M.C., A.S., G.C., CC.Y, M.D., B.H. H.J. U.S. All authors approved the final version of the manuscript. The authors have no conflict of interest to disclose.

Acknowledgements

This work was supported by Deutsche Forschungsgemeinschaft grant nos SFB621-C9, Se460/9-5 and Se460/9-6 (to U.S.), the Volkswagen Vorab-Stiftung, the Hannover Biomedical Research School and the PhD program 'Molecular Medicine' with a stipend to M.C., A.S. and A.S. We thank Regina Engelhardt, Brigitte Rausch and Natascha Cirpka for their help with the animal breeding and genotyping.

Author's present address

B. Hogema: The Sanquin blood supply foundation, Plesmanlaan 125, 1066 CX Amsterdam, The Netherlands.